



**Acoustics'08
Paris**
June 29-July 4, 2008
www.acoustics08-paris.org

Frequency sweeping and fluid flow effects on particle trajectories in ultrasonic standing waves

Bart Lipkens^a, Jason Dionne^a, Michael Costolo^b and Edward Rietman^b

^aWestern New England College, 1215 Wilbraham Road, Box S-5024, Springfield, MA 01119, USA

^bPhysical Sciences Inc., 20 New England Business Center, Andover, MA 01810, USA
blipkens@wnec.edu

Particle concentration in ultrasonic standing waves by the acoustic radiation force is discussed. The acoustic radiation force is a function of the density and compressibility of the fluid and the suspended particles. A two-dimensional theoretical model is developed for particle trajectory calculations. An electro-acoustic model is used to predict the acoustic field in a resonator. The results of the linear acoustic model are used to calculate the acoustic radiation force acting on a particle suspended in the resonator. A particle trajectory model is developed that integrates the equation of motion of a particle subjected to a buoyancy force, a fluid drag force, and the acoustic radiation force. Computational fluid dynamics simulations are performed to calculate the velocity field. For a fixed frequency excitation, the particles are concentrated along the stable node locations of the acoustic radiation force. Through a periodic sweeping of the excitation frequency particle translation is achieved. Two types of frequency sweeps are considered, a ramp approach and a step-change method. Numerical results of particle trajectory calculations in a resonator with dimensions much larger than a typical wavelength are presented. Experimental observations of particle concentration of 6 μm polystyrene spheres are presented.

1 Introduction

Trajectories of particles, subjected to several forces, such as the buoyancy force, the fluid drag force, and the acoustic radiation force, are numerically calculated. The model is used as a design tool of flow-through resonators with inlets and outlets for fluid flow to enter and exit the resonator. The fluid flow entering the waveguide contains suspended particles that need to be filtered from the fluid flow. The action of the acoustic radiation force concentrates and separates these particles from the fluid stream. For a fixed frequency excitation, the action of the acoustic radiation force moves the particles to the stable zero locations of the acoustic radiation force. Drifting ultrasonic waves, created by a periodic sweeping of the excitation frequency, are used to achieve particle translation across portions of the resonator.

Several review papers [1] – [5] present an overview of the fundamental principles and applications of the acoustic radiation force. King [6], Yosioka and Kawasima [7], Gor'kov, [8] and others developed the fundamental theories of the acoustic radiation force. Of interest to our current efforts is the work by Tolt and Feke [9], [10]. They developed a separation process based on the acoustic radiation force in a stationary ultrasonic standing wave field. They employed a forced coincidence excitation method where flexural wave modes of the pipe wall (in which the fluid resides) are matched with higher order acoustic modes of the fluid within the pipe. Tolt and Feke [9] used a frequency sweeping method to translate the concentrated particles across the resonator. The frequency sweep is over a range of $2f_0$, where f_0 is the fundamental resonance frequency of a resonator with length L , i.e., $f_0=2c_f/L$, where c_f is the speed of sound of the fluid in the resonator. Hill et al. [11, 12] and Townsend et al. [13] developed a model for the calculation of particle paths for suspended particles in a fluid. The particles are exposed to three forces, acoustic radiation force, fluid drag force, and buoyancy force. An electro-acoustic model is used to calculate the acoustic field in the resonator. A separate model is used to calculate the flow velocity vectors in the resonator. A third model considers the particle-acoustic field interaction. Harris et al. [14] used a similar model as that described by Hill [11] to calculate the performance of a micro-engineered ultrasonic particle manipulator. Results from the model were compared with experimental results for separation of 1 μm latex particles and yeast particles in

water. A second example of using frequency sweeps to translate particles across an ultrasonic resonator is presented in the work by Handl et al. [15]. They used a four step frequency sweep that alternated between the frequencies of four consecutive acoustic resonance frequencies of the cavity. They showed that under these conditions particles are translated across the resonator. The measured particle trajectories compared favorably with those predicted by a numerical model.

The goal of this work is to develop an engineering design model for the calculation of particle trajectories in the presence of fluid drag, buoyancy, and acoustic radiation force. The resonators are macro-scale cavities, typically about 0.15m long, and 0.03x0.03m in cross-section. Flow inlets and outlets are connected to the resonator. Laminar flow fields are assumed. The goal is to design resonators for the concentration and separation of particles from a particle-laden inlet flow. Typically, two outlets are configured, one for the particle-free fluid and another for the particle rich fluid stream. Particles are concentrated and then translated across the resonator by the acoustic radiation force. Translation occurs through a periodic sweeping of the frequency of excitation, similar to Tolt and Feke [9] and Handl et al. [15]. The numerical model consists of multiple sub-models and uses the same framework as developed by Hill et al. [11, 12] and Townsend et al. [13]. A first model is the electro-acoustic model of a multi-layered resonator. The second model is that of the particle – acoustic field interaction. The third model is a computational fluid dynamics (CFD) simulation of the steady flow field in the inlet, resonator, and outlets of the system. The fourth model integrates the equations of motion of a particle in the resonator. Three forces act on the particle: the acoustic radiation force, the buoyancy force, and the fluid drag force.

In section 2, the electro-acoustic model and the acoustic radiation force model are discussed. Section 3 covers the CFD simulation and the particle trajectory model. Results of the electro-acoustic model are shown in section 4. Particle trajectory computations and experimental results are shown in section 5.

2 Electro-acoustic model

A one dimensional model of the acoustic pressure and velocity in a particle concentrator has been developed. It includes the coupling with a piezoelectric transducer. Hence, it allows for the direct calculation of acoustic

pressure as a function of the applied voltage to the transducer. As such it can be used to study the effect of the inclusion of matching layers, the type of bonding materials used, and the geometry and type of material of the end cap of the concentrator. Once the acoustic field is solved for, the acoustic radiation force is calculated through a numerical implementation of Gorkov's expression [8] for the radiation force. The basic setup of the model is similar to that of Hill et al. [11, 12] and Townsend et al. [13].

2.1 Acoustic model

The acoustic pressure and velocity in a material layer is calculated as function of the end impedance of the layer and the properties of the layer, i.e., density ρ , speed of sound c , and frequency f . Fig. 1 shows a schematic of a typical material layer. The mechanical impedance at the end of the layer is denoted by Z_{mL} , where the mechanical impedance is defined as $Z_m = F/u = P \cdot S / u$, the ratio of force divided by velocity, where the force F is the product of pressure P and cross-sectional area S . One dimensional wave propagation is

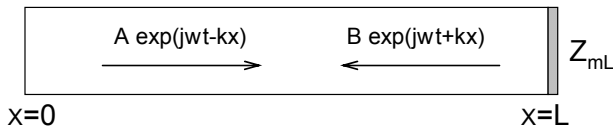


Fig. 1. Schematic of an acoustic waveguide terminated by a mechanical impedance Z_{mL} . A is the amplitude of the forward propagating wave, and B the amplitude of the backward propagating wave.

used where the forward propagating pressure wave is defined as $A \exp(j\omega t - kx)$ and the backward propagating wave is defined as $B \exp(j\omega t + kx)$. A and B are the magnitudes of the pressure waves, ω is the angular frequency, $k = \omega/c$ is the wavenumber, and c is the speed of sound. The total pressure in the layer is then

$$p(x, t) = A e^{j\omega t} \left[e^{-jkx} + \frac{B}{A} e^{jkx} \right], \quad (1)$$

and the particle velocity u is found from the linearized momentum equation as

$$u(x, t) = \frac{A}{\rho c} e^{j\omega t} \left[e^{-jkx} - \frac{B}{A} e^{jkx} \right]. \quad (2)$$

The mechanical impedance is then given by

$$Z_m(x) = \rho c S \frac{\left[e^{-jkx} + \frac{B}{A} e^{jkx} \right]}{\left[e^{-jkx} - \frac{B}{A} e^{jkx} \right]}. \quad (3)$$

By applying the known end impedance Z_{mL} , we find the following equations for the impedance Z_m , acoustic pressure $p(x, t)$, and particle velocity $u(x, t)$ in the resonator,

$$Z_m(x) = \rho c S \frac{\left[\frac{Z_{mL}}{\rho c S} + j \tan k(L-x) \right]}{\left[1 + j \frac{Z_{mL}}{\rho c S} \tan k(L-x) \right]}, \quad (4)$$

$$p(x, t) = \frac{2A}{\frac{Z_{mL}}{\rho c S} + 1} e^{j(\omega t - kL)} * \left[\frac{Z_{mL}}{\rho c S} \cos k(L-x) + j \sin k(L-x) \right], \quad (5)$$

and

$$u(x, t) = \frac{2A}{\frac{Z_{mL}}{\rho c S} + 1} e^{j(\omega t - kL)} * \left[\cos k(L-x) + j \frac{Z_{mL}}{\rho c S} \sin k(L-x) \right]. \quad (6)$$

These equations can now be repeatedly used for a typical concentrator cell that contains many layers.

Losses can be included in the model by incorporating complex material constants.

2.2 Piezo-electric transduction model

A transducer model operates in its thickness mode near its resonance frequency. Standard piezo-electric relations provide the coupled equations that describe the operation of the transducer. A general representation of the mechanical impedance Z_m of the piezoelectric transducer includes a mass M_m , compliance C_m , and a damper R_m , or

$$Z_m = j\omega M_m + \frac{1}{j\omega C_m} + R_m. \quad (7)$$

To obtain a complete circuit representing the piezoelectric transducer and the load that the transducer drives, we include a supply voltage E_o and internal impedance Z_g representing the voltage from the amplifier driving the transducer and a load impedance Z_L which represents the mechanical impedance of the concentrator cell acting on the transducer. The load impedance can be calculated by following the procedure discussed in the previous section. This final circuit is shown in Fig. 3, where α_{em} is the electro-mechanical coupling factor and C_e is the electrical capacitance of the transducer.

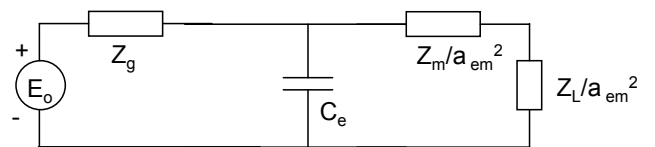


Fig. 3. Complete circuit representation of the piezoelectric transducer, including the amplifier that supplies the voltage to the circuit and the mechanical load impedance presented by the concentrator cell.

The circuit is solved for the voltage across the load impedance which is related to the force F_1 acting at the interface between the transducer and the first layer. The result for the force is

$$F_1 = \frac{\alpha_{em} Z_L E_o}{Z_m + Z_L + Z_g \left(j\omega C_e [Z_m + Z_L] + \alpha_{em}^2 \right)}. \quad (8)$$

Once the force F_1 between the transducer and the first layer is found from (8), we can use (5) to solve for the unknown amplitude A and then to determine the force F_L at

the end of the first layer, at the interface between layer one and two. This force is given as

$$F_L = \frac{Z_{mL} F_1}{Z_{mL} \cos kL + j\rho c S \sin kL}, \quad (9)$$

where Z_{mL} is the mechanical impedance at the end of the layer and the layer length is L . Repeated application of (9) yields the forces at the interfaces. The variation of pressure and velocity in each layer can be calculated in a similar way. The result is

$$p(x,t) = \frac{F_1}{S} \left[\frac{Z_{mL} \cos k(L-x) + j\rho c S \sin k(L-x)}{Z_{mL} \cos kL + j\rho c S \sin kL} \right] \quad (10)$$

and

$$u(x,t) = \frac{F_1}{\rho c S} \left[\frac{\rho c S \cos k(L-x) + jZ_{mL} \sin k(L-x)}{Z_{mL} \cos kL + j\rho c S \sin kL} \right], \quad (11)$$

where F_1 is the force at the $x=0$ interface of the layer.

2.3 Acoustic radiation force

Next, the acoustic radiation force is calculated according to the formulation of Gor'kov [8]. The primary acoustic radiation force F_A is defined as a function of a field potential U

$$F_A = -\nabla(U), \quad (12)$$

where the field potential U is defined as

$$U = V_0 \left[\frac{\langle p^2(x,y,t) \rangle}{2\rho_f c_f^2} f_1 - \frac{3\rho_f \langle u^2(x,y,t) \rangle}{4} f_2 \right], \quad (13)$$

and f_1 and f_2 are the monopole and dipole contributions defined by

$$f_1 = 1 - \frac{1}{\Lambda \sigma^2}, \quad (14)$$

$$f_2 = \frac{2(\Lambda - 1)}{2\Lambda + 1}$$

where $p(x,y,t)$ is the acoustic pressure and $u(x,y,t)$ is the fluid particle velocity. Λ is the ratio of particle density ρ_p to fluid density ρ_f and σ is the square of the ratio of particle sound speed c_p to fluid sound speed c_f . V_0 is the volume of the particle. For a one-dimensional harmonic acoustic wave, the expression for the acoustic radiation force is:

$$F_{Ax} = V_0 \left[\frac{3(\rho_p - \rho_f) \rho_f}{2\rho_p + \rho_f} U_M \frac{dU_M}{dx} \right] - \quad (15)$$

$$V_0 \left[\left(1 - \frac{\rho_f c_f^2}{\rho_p c_p^2} \right) \frac{1}{2\rho_f c_f^2} P_M \frac{dP_M}{dx} \right],$$

where U_M and P_M are the magnitudes of acoustic velocity and pressure. The calculation of the acoustic radiation force is implemented through a numerical calculation of the spatial derivative of velocity and pressure.

3 Particle trajectory model

The particle trajectory model contains the algorithm to calculate the trajectories of particles entering the acoustic concentrator cell from the inlet port. The model takes into account three forces acting on the particles, (1) the fluid drag force, (2) the buoyancy force, and (3) the acoustic radiation force

The particle trajectory model that is developed is a two-dimensional model of the concentrator. The x-axis represents the horizontal dimension along which the acoustic radiation force acts and the y-axis is the vertical dimension. The equations that govern the trajectories of the particles are

$$\frac{d^2 x_p}{dt^2} = \frac{F_{Dx} + F_{Ax}}{m_p} \quad (16)$$

$$\frac{d^2 y_p}{dt^2} = \frac{F_{Dy} + F_B}{m_p}.$$

Here x_p and y_p represent the location of a particle of mass m_p at a given time t . The fluid drag force is F_D , the acoustic radiation force is F_A , and the buoyancy force is F_B . The equations are integrated numerically with a fourth-order integration scheme with variable time step. A typical value for the minimum time step is on the order of 0.1 μ s. In the current model the y-axis is always assumed to be the vertical axis. Therefore, the buoyancy force only acts in the y-direction. The acoustic radiation force only acts in the x-direction. It is straightforward to generalize the model and incorporate components of the acoustic radiation force and the buoyancy force in the both directions.

The fluid drag force F_D is given by

$$F_D = 6\pi\mu R_p (u_f - u_p), \quad (17)$$

where R_p is the particle radius, u_f is the fluid velocity, u_p is the particle velocity, and μ is the dynamic viscosity.

In order to calculate the fluid drag force we have to calculate the flow field in the concentrator. This is done by a CFD simulation. Fluent is used for the CFD calculations. Once a solution is obtained, the entire velocity flow field is saved, i.e., all the velocity vectors at all the grid points are saved to a file. The particle tracer model includes a bilinear interpolation routine to find the flow velocity vector at any point within the concentrator cell.

The buoyancy force F_B is given by

$$F_{By} = \frac{4}{3} \pi R_p^3 g (\rho_f - \rho_p), \quad (18)$$

where g is the gravitational acceleration.

4 Results of electro-acoustic model

The model was used to predict the performance of a 15 cm long glass concentrator cell. The cell has a diameter of 1.125 inches. The cell is capped at one end with a 2 MHz PZT4 transducer of 1" diameter. The other end is capped with an Aluminum end cap. The thickness of the end-cap is made to be one quarter of the operating wavelength of the cell. Standard properties of PZT-4 are used to calculate the

characteristics of the transducer. For a 15 cm water column, the fundamental resonance frequency is 4.921 kHz. The frequency response of the peak acoustic pressure in the resonator is shown for frequencies near the transducer resonance.

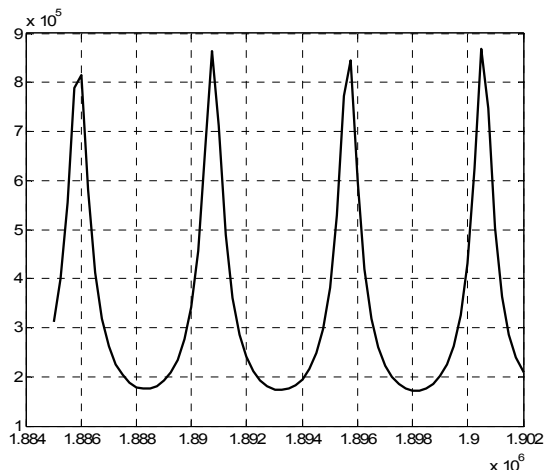


Fig. 4. Frequency response function of the peak acoustic pressure in the resonator, showing acoustic pressure (Pa) versus time (s). Calculations are done for a 55V supply voltage.

5 Particle trajectories

5.1 Zero mean fluid flow trajectories

Simulations were done for a particle with a density of 1100 kg/m^3 , a speed of sound of 2400 m/s , and a radius of $3 \text{ }\mu\text{m}$. The particle simulations were done for a four level backward frequency sweep, i.e., 1.8860, 1.8908, 1.8958, and 1.9008 MHz . The sweep period is 0.08s . The particle simulation is done for a particle that is initially located at a distance of 0.04m from the transducer face. As shown in Figure 5, initially the particle moves to the left to its stable location, then, switching to the next frequency initiates translation of the particle to the right. It takes about 0.02s for the particle to reach its equilibrium position at about 0.03993m . A simulation was done for a total time duration of 0.8s . The results are shown in Figure 6 and indicate that over the entire duration of the simulation (0.8s) the particle translates over a distance of 2.7mm , resulting in an average translation speed of 3.375mm/s .

Experiments were performed in a 6 inch long glass tube driven by a 2 MHz piezo-transducer. A similar sweeping method was used to concentrate and translate the $6 \text{ }\mu\text{m}$ polystyrene spheres. Fig. 7 shows the concentrated particles. Fig. 8 shows the particle location after several minutes of exposure to the ultrasound. As can be seen, the particles have translated to the top of the resonator and form a large clump.

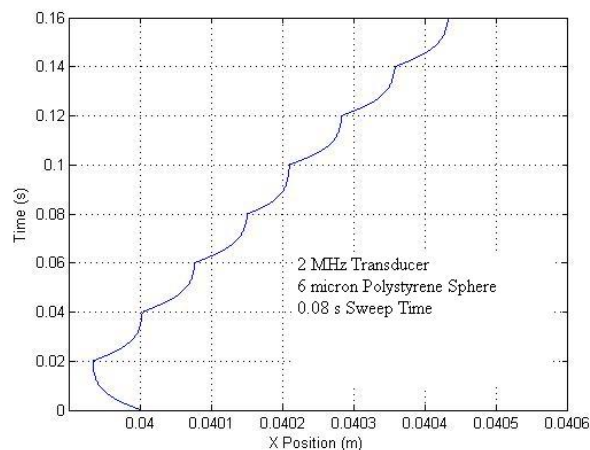


Fig. 5. Calculated particle trajectory for a $6 \text{ }\mu\text{m}$ polystyrene particle for a two sweep period time window.

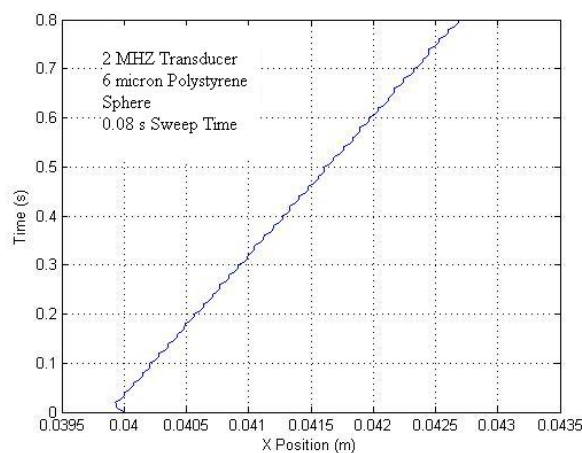


Fig. 6. Calculated particle trajectory for a $6 \text{ }\mu\text{m}$ polystyrene sphere over a 0.8s time window.

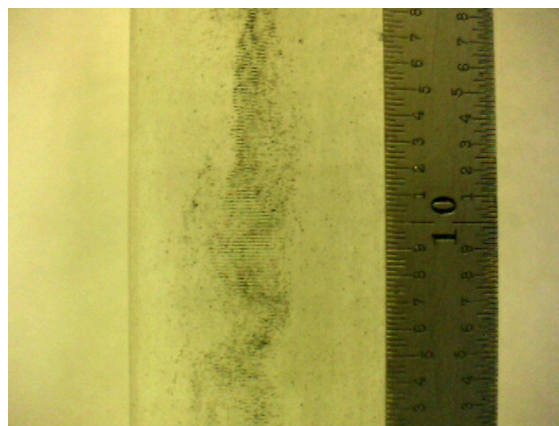


Fig. 7. Photo of concentrated $6 \text{ }\mu\text{m}$ polystyrene spheres. Transducer frequency is 2 MHz .

5.2 Particle trajectories in presence of mean fluid flow

An example of a typical result for particle translation in the presence of mean flow is shown in Fig. 9. There is a laminar flow field entering the resonator at the top. The flow field is split into two streams, a wider stream for the cleaned fluid, and a smaller collector stream for the captured particles. The average inlet flow velocity is 8.5 mm/s . A particle trajectory is shown for a particle that is located in the inlet channel near the left wall. As can be

seen through the action of the acoustic radiation force the particle is able to move across the primary stream, so that it is collected by the secondary stream.

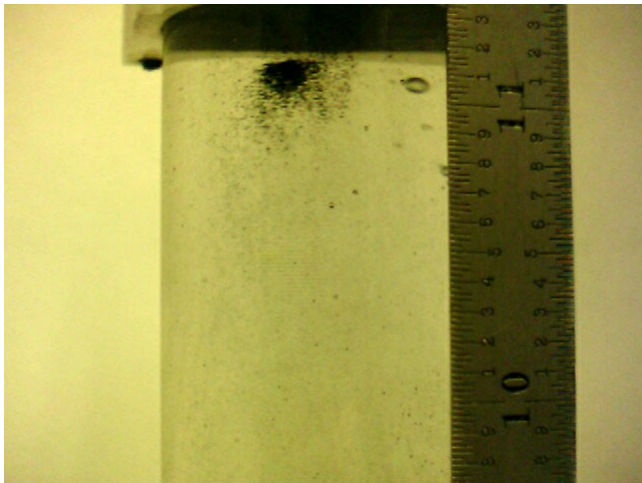


Fig. 8. Photo of 6 μm polystyrene spheres that have translated to the top of the 6 inch resonator. Frequency of excitation is 2 MHz.

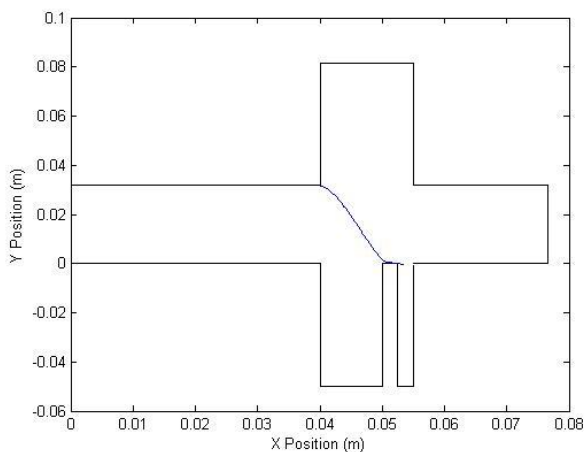


Fig. 9. Example of particle trajectory calculation in the presence of mean flow.

6 Conclusion

A model is developed for particle trajectory calculations in a fluid. The particle is subjected to three forces, buoyancy, fluid drag, and the acoustic radiation force. A numerical integration is used to determine the particle trajectories.

Particle translation is achieved through a periodic sweeping of the frequency of excitation. Linear frequency sweeps results in particles translated from one end of the resonator to a location near the other end.

The simulations show that particle separation processes that use the acoustic radiation force can be effective in removing particles from an inlet stream in a flow-through device.

Acknowledgments

This work was funded by the U.S. Army under STTR contract number W911SR-06-C-0040. We thank Dr. James

Jensen for technical discussions.

References

- [1] P. L. Marston and D. B. Thiessen, "Manipulation of fluid objects with acoustic radiation pressure," *Ann. N. Y. Acad. Sci.*, vol. 1027, pp. 414-434, 2004
- [2] T. G. Wang and C. P. Lee, "Radiation pressure and acoustic levitation," in *Nonlinear Acoustics*, M. F. Hamilton & D. T. Blackstock, Eds. Academic Press, San Diego, 1998.
- [3] R. E. Apfel, "Radiation pressure – principles and application to separation science," *Fortschritte der Acustik DAGA*, pp. 19-36, Wien, 1990.
- [4] M. Groschl, "Ultrasonic separation of suspended particles – part I: fundamentals," *Acustica*, vol. 84, no. 3, pp. 432-447, 1998.
- [5] M. Groschl, "Ultrasonic separation of suspended particles – part II: design and operation of separation devices," *Acustica*, vol. 84, no. 4, pp. 632-642, 1998
- [6] L. V. King, "On the acoustic radiation pressure on spheres," *Proc. R. Soc. London, Ser. A*, vol. 147, pp. 212-240, 1934.
- [7] K. Yosioka and Y. Kawasima, "Acoustic radiation pressure on a compressible sphere," *Acustica*, vol. 5, pp. 167-173, 1955.
- [8] L. P. Gor'kov, "On the forces acting on a small particle in an acoustical field in an ideal fluid," *Sov. Phys. Dokl.*, vol. 6, pp. 773-775, 1962.
- [9] T. L. Tolt and D. L. Feke, "Separation devices based on forced coincidence response of fluid-filled pipes," *J. Acoust. Soc. Am.*, vol. 91 no.6, pp. 3152-3156, 1992.
- [10] T. L. Tolt and D. L. Feke, "Separation of dispersed phases from liquids in acoustically driven chambers," *Chem. Eng. Sci.*, vol. 48, no. 20, pp. 527, 1993.
- [11] M. Hill and R. J. K. Wood, "Modelling in the design of a flow-through ultrasonic separator," *Ultrasonics*, vol. 38, pp. 662-665, 2000.
- [12] M. Hill, Y. Shen, and J. J. Hawkes, "Modelling of layered resonators for ultrasonic separation," *Ultrasonics*, vol. 40, pp. 385-392, 2002.
- [13] R. J. Townsend, M. Hill, N. R. Harris, and N. M. White, "Modelling of particle paths passing through an ultrasonic standing wave," *Ultrasonics*, vol. 42, pp. 319-324, 2004.
- [14] N. R. Harris, M. Hill, R. Townsend, N. M. White, and S. P. Beeby, "Performance of a micro-engineered ultrasonic particle manipulator," *Sensors and Actuators B*, vol. 111-112, pp. 481-486, 2005.
- [15] B. Handl, M. Groschl, F. Trampler, E. Benes, S. M. Woodside, and J. M. Piret, "Particle trajectories in a drifting resonance field separation device," *Proc. of the 16th Int. Congress on Acoustics and 135th Meeting of the Acoust. Soc. Am.*, ISBN 1-56396-817-7, vol. III, pp. 1957-1958, 1998.